Nonlinear Optics and Quantum Optics, Vol. 40, pp. 95–113
Reprints available directly from the publisher
Photocopying permitted by license only

Nonlinear Absorption Spectroscopy of Organic Dyes

ERIC W. VAN STRYLAND[1], DAVID J. HAGAN[1], OLGA V. PRZHONSKA[1,2]
SETH R. MARDER[3], SCOTT WEBSTER[1] AND LAZARO A. PADILHA[1]

[1]*CREOL, The College of Optics and Photonics, University of Central Florida, 4000 Central Florida Blvd., Orlando, Florida 32816–2700 USA*
E-mail: ewvs@creol.ucf.edu
[2]*Institute of Physics, National Academy of Sciences, 46 Prospect Nauki, Kiev 03028 Ukraine*
[3]*Center for Organic Photonics and Electronics and School of Chemistry and Biochemistry, Georgia Institute of Technology, 911 Atlantic Dr., Atlanta, GA 30332–0400 USA*

Received: November 4, 2009. Accepted: December 1, 2009.

We perform nonlinear spectroscopic measurements on organics materials with the aim of building a database of nonlinear optical parameters to aid in investigating and developing new experimental techniques and theories. Through years of collaboration, our groups have developed several experimental techniques and apparatus' which have been precursors to developing a true nonlinear optical spectrophotometer needed to understand complex photophysical and photochemical processes. With these techniques, including: open- and closed-aperture Z-scan; white-light-continuum (WLC) Z-scan; one- and two-photon fluorescence; emission and excitation anisotropy; direct luminescence lifetime measurements; and femtosecond-pump WLC-probe spectroscopy, we have investigated many unique classes of organic dyes with nonlinear responses due to two- and three-photon absorption, excited-state absorption induced by one- and multi-photon absorption, and combinations of these processes. By performing both experiment and modeling, including quantum chemical calculations, determining both frequency degenerate and non-degenerate spectra along with their associated temporal dynamics, the responsible physical mechanisms can be determined. Additionally, we are studying the nonlinear refraction of these materials and the observed nonlinear responses, both absorptive and refractive, which mirror those observed in bulk semiconductors with relatively minor differences). This allows us to apply our experience and previously developed theories of modeling semiconductors to organics. Working in collaboration with optical scientists, physicists, materials scientists, and chemists has greatly increased our progress towards predictive structure-property relations in organics.

Keywords: Nonlinear optics, absorption, refraction, organics, Z-scan, white-light continuum, structure-property relations.

INTRODUCTION

In this paper, we briefly summarize the techniques that we have developed over the past several years to elucidate various nonlinear optical (NLO) responses, specifically those involving nonlinear absorption and refraction occurring in organic materials. We then show how we use these techniques to measure the ultrafast and cumulative nonlinear responses of a variety of representative materials, many of which exhibit large NLO responses. We compare these responses to analogous responses in bulk semiconductors and examine figures of merit for all-optical switching. We conclude by noting that larger nonlinear optical responses are necessary for many practical NLO device applications. The development of a large and reliable database is needed to more fully understand the relationships between NLO properties and molecular structure.

NONLINEAR SPECTROSCOPIC TECHNIQUES

Z-scan

The original Z-scan technique, introduced in 1989 [1], involves axially translating a sample through the focus of a Gaussian spatial and temporal beam profile (although Gaussian profiles are not necessary, modeling the results is greatly simplified) while monitoring the transmitted light. Often, a beam splitter is placed after the sample to split the transmitted beam onto two detectors. The first detector measures the total transmitted light, and is commonly referred to as an open-aperture Z-scan. The second beam is then apertured in the far-field, typically using an iris diaphragm closed to $\sim$40% linear transmittance (this averages beam spatial inhomogeneities without sacrificing much sensitivity), and then is collected onto a second detector. This is commonly referred to as a closed-aperture Z-scan. Figure 1 shows these two experiments separately along with representative signals. The open-aperture Z-scan is only sensitive to nonlinear absorption as long as the sample is thin compared to the Rayleigh range and thin enough that phase changes do not propagate to beam distortion within the sample. The closed-aperture Z-scan is sensitive to both nonlinear refraction and absorption; however, if the closed-aperture signal is divided by the open-aperture signal, the resulting signal is nearly identical to the signal that would have been obtained without the nonlinear absorption loss. This simplifies the data analysis when the nonlinear absorption is smaller or comparable to the change in transmittance from nonlinear refraction, otherwise a more sophisticated method must be employed to model the signals numerically [2]. This simplicity of separating absorptive and refractive nonlinearities is one of the attributes that has made Z-scan so popular [3].

Another aspect of the Z-scan technique is its remarkable sensitivity to induced phase distortion. We have performed Z-scans with sensitivity to $\lambda/10^3$ (the "EZ-scan", which uses a stop in place of the aperture, has shown

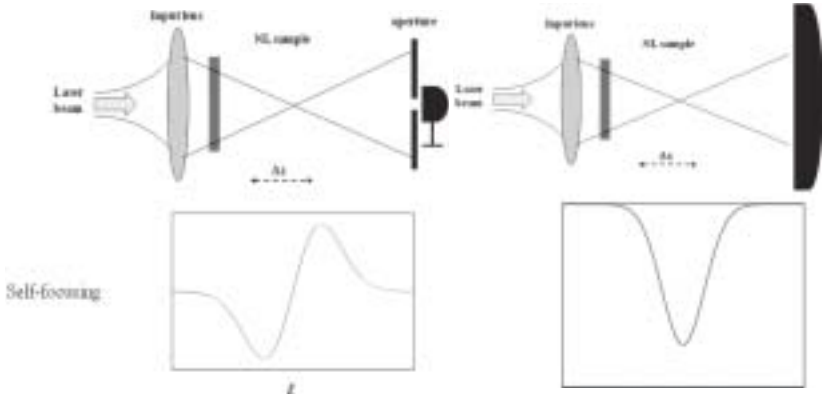

FIGURE 1
(Left) "Closed-aperture" Z-Scan and the resulting signal for a third-order self-focusing nonlinear response. (Right) "Open-aperture" Z-Scan and the resulting signal for a third-order nonlinear response.

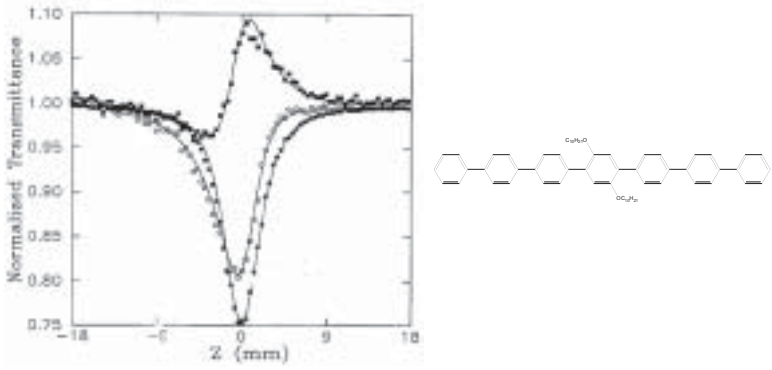

FIGURE 2
Open (open circles), closed (closed circles) and divided (closed squares) Z-scan data of the organic molecule (shown above). The solid lines are fits to the data. From Ref. [5].

sensitivity to $\lambda/10^4$) [4]. This interferometric-like sensitivity may at first seem odd for a technique using a single beam; however, the sample serves as a phase mask, and the amplitude distortion appears upon propagation to the far field, i.e. via diffraction. In reality, diffraction is an interference phenomenon between different spatial portions of the beam. It is useful to think of the high intensity center interfering with the low intensity wings of the beam. Thus, the Z-scan technique is a single beam interference method without the alignment complexities of other interferometers.

Shown in Fig. 2 are examples of nonlinear signals obtained by the Z-scan technique for a simple organic structure. The nonlinear response is initiated by two-photon absorption (2PA) and then the excited states produced by 2PA

linearly absorb. This process is commonly referred to as 2PA-induced excited-state absorption (ESA). Associated with the 2PA is a bound electronic nonlinear refraction, n_2, and associated with the creation of excited-state absorbers is a change in index proportional to the density of these excited states. All of these mechanisms are needed to fit these data. The nonlinear transmittance, as measured by the open-aperture Z-scan can be modeled according to,

$$\frac{dI(t)}{dz} = -\alpha_2 I^2(t) - \sigma_{ex} N(t) I(t), \tag{1}$$

where α_2 is the 2-photon absorption coefficient, σ_{ex} is the excited-state absorption coefficient and N is the density of excited states produced by two-photon absorption, given by,

$$\frac{dN}{dt} = \frac{\alpha_2 I^2(t)}{2\hbar\omega}. \tag{2}$$

For molecules, the 2PA is often expressed in terms of a 2PA cross section, given by, $\delta \equiv \frac{\hbar\omega}{N}\alpha_2$. By analogy, we define the nonlinear refractive cross section in terms of n_2 by: $\delta_r \equiv \frac{\hbar\omega}{N} k_0 n_2$. Both have units of GM.

Similarly, the nonlinear phase shift, $\varphi(z, t)$ is determined by

$$\frac{d\phi(z, t)}{dz} = n_2 I(z, t) + \sigma_R N(z, t), \tag{3}$$

where n_2 is the coefficient of instantaneous nonlinear refraction due to the dye plus solvent and σ_R is the refractive index per excited state per unit volume. Since N is proportional to the square of the irradiance, the excited-state absorption and refraction are higher order nonlinearities than the 2PA and n_2, and hence we can separate these effects by performing Z-scans at several irradiances.

Determining a complete spectrum by changing input wavelengths can be a time consuming process. Typically, the source alignment needs to be adjusted, and optics and detectors may need to be changed forcing the re-alignment of the setup. Complete nonlinear spectroscopy becomes very tedious, but still possible, as seen in Fig. 3 [6].

Determining the physical mechanism or mechanisms responsible for the signal is seldom (if ever) revealed by a single Z-scan experiment [7]. Figure 4 shows data obtained on a sample of chloro-aluminum phthalocyanine (CAP) using a fixed energy but pulse widths differing by a factor of two [8]. Thus the irradiance changes by a factor of two while the signals for both nonlinear absorption and nonlinear refraction are nearly identical. Clearly this cannot be from 2PA.

What we can determine from these data along with pump-probe data discussed below, is that this molecule shows ESA along with the associated nonlinear refraction due to redistributing the populations of the molecular states. The equations describing the absorption and phase change induced on

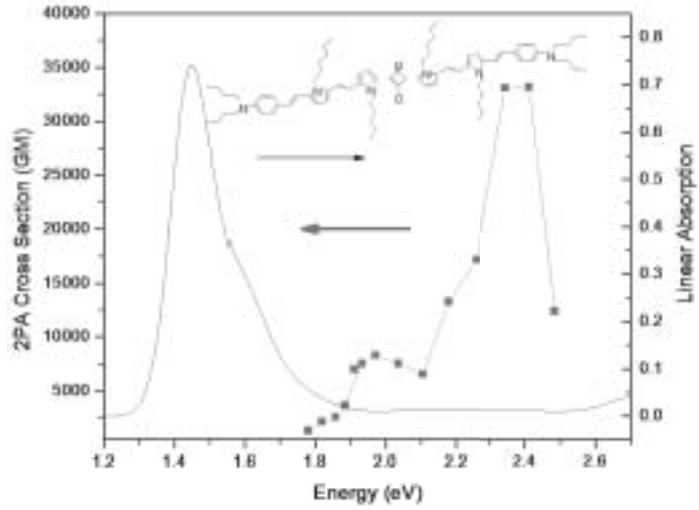

FIGURE 3
Linear absorption (right axis) along with 2PA cross section (left axis) versus energy for the molecule shown. The energy corresponds to the energy of final excitation for both linear and two-photon absorption, e.g. the 2PA peak is near an input photon energy of 2.35/2 eV.

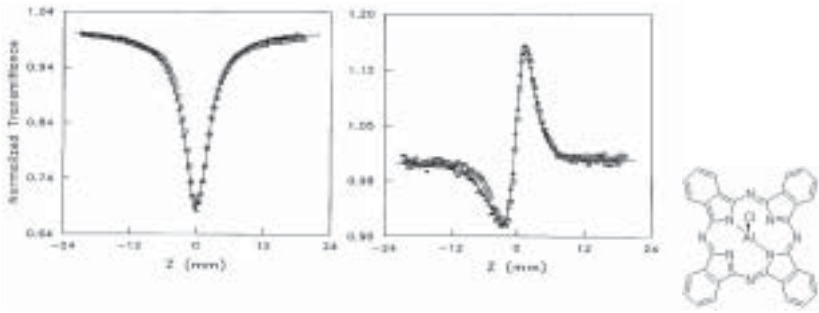

FIGURE 4
Open aperture Z-scan data at 532 nm using (Δ) 30 ps pulses (FWHM), and (□) 62 ps pulses (FWHM) on CAP – left, and closed aperture Z-scan data (divided by open aperture data) for the same pulsewidths – right. The molecule is shown at the right. From Ref. [8].

the incident beam by these phenomena using a 3-level system as shown in Fig. 5, are:

$$\frac{dI}{dz} = -\sigma_g N_g I - \sigma_{ex} N_{ex} I; \quad \frac{dN_{ex}}{dt} = \frac{\sigma_g N_g I}{\hbar\omega} - \frac{N_{ex}}{t_1}; \quad \frac{d\phi}{dz} = \sigma_R N_{ex}, \quad (4)$$

where σ_g and σ_{ex} are the absorption cross sections of the ground and excited state (cm^2), N_x are the corresponding molecular densities (cm^{-3}), t_1 is the excited state lifetime (s), and σ_R is the excited-state refractive cross section (cm^2), and the total molecular density is assumed to be the sum of the ground

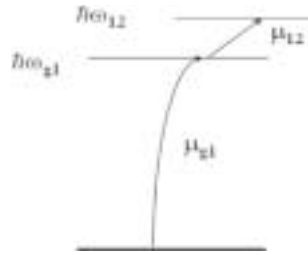

FIGURE 5
3-level model describing both ESA (when $\hbar\omega_{12} \sim \hbar\omega_{g1}$), and 2PA when the intermediate state is far from linear absorption resonance as shown in the figure.

and excited-state molecular densities. Any higher excited state is assumed to decay very rapidly; usually a good approximation.

If the lifetime $t_1$is long (here $\gg$ 60 ps) compared to the pulsewidth, the second term in the second equation can be ignored. This allows us to temporally integrate the first two equations to obtain the following equation describing the loss of fluence, F (J/cm^2), with distance:

$$\frac{dF(t)}{dz} = -\sigma_g NF(t) - N\frac{\sigma_g\sigma_{ex}}{2\hbar\omega}F^2(t). \tag{5}$$

This equation is nearly identical to the equation describing the loss of irradiance for 2PA if there is some residual linear loss α, i.e.

$$\frac{dI(t)}{dz} = -\alpha I(t) - \alpha_2 I^2(t) \tag{6}$$

where α is the linear absorption coefficient, except that the fluence is replaced by irradiance and α_2 is given by a product of linear absorption cross sections and the molecular density. This shows us how resonant two-photon absorption, i.e. ESA, is closely related to nonresonant 2PA. Perturbation theory (see Ref. [9]), gives a molecular 2PA cross section that is proportional to the products of the squares of transition dipole moments between ground and first excited and first excited and second excited states, i.e. $\alpha_2 \propto |\mu_{g1}|^2|\mu_{12}|^2$. These squares of transition dipole moments are each proportional to their respective linear absorption cross sections, σ_x.

The determination of the nonlinear mechanisms involved with a specific material is not solely determined by the Z-scan since it is sensitive to all NLO absorptive and refractive effects. Other data is needed. One of the primary methods to help determine the physics of the nonlinear response is its temporal dependence. This can be determined by pump-probe methods which we discuss next [10].

Pump-probe method

Figure 6 shows the standard pump-probe experimental setup where a pump excites the system at time $\tau = 0$ and the probe examines the change in

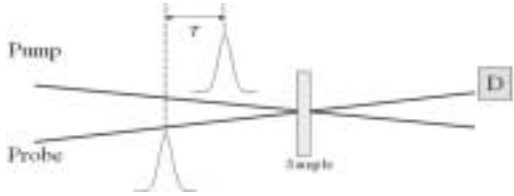

FIGURE 6
Pump-probe experimental setup.

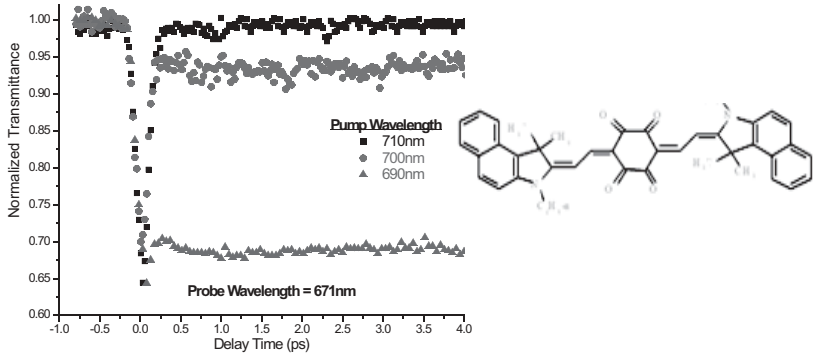

FIGURE 7
Normalized transmittance of a sample shown as a function of the probe time delay after excitation by a ∼150 fs pump pulse at the three wavelengths shown. The probe pulse is set at 671 nm. From Ref. [11].

transmission properties of the sample at later times $\tau > 0$ [10]. Here the pump and probe can be at different frequencies.

ESA can easily be differentiated from 2PA by this technique since for times after short pulse excitation (pulsewidth shorter than the decay time of the system, e.g. t_1 in Eq. 1) the excited-state absorption will be present after the excitation pulse is over, i.e. for τ greater than the pulsewidth. In Fig. 7 we show a more complicated situation where excited states are created by 2PA as opposed to linear absorption (this was also the case for the molecule and data shown in Fig. 2). These are also seen by the presence of the excited-state absorption lasting for times long compared to the pulsewidth.

A Z-scan of the nonlinear absorption at wavelengths in this range would show a combination of 2PA and the higher-order nonlinear absorption from the 2PA generated excited states. This is shown in Fig. 8 where the 2PA cross section spectrum of the same organic molecule is shown using multiple techniques, two-photon fluorescence [12] and Z-scan.

At around 690 nm the Z-scan gives an "effective" cross section of ∼35,000 GM; however, much of this is actually due to ESA so that the corrected 2PA cross section is ∼13,000 GM as noted on the figure [12]. This was not the case with the sample of Fig. 3 where it was checked that this was entirely

due to 2PA. Performing nonlinear spectroscopy with the Z-scan using tunable sources such as optical parametric devices is quite time consuming since after each tuning the pulses must usually be spatially filtered and completely characterized in terms of spatial profile and temporal profile. We will discuss an interesting variation on the usual Z-scan utilizing a high brightness white-light continuum in the section on "WLC Z-scan"; however, first we will show a rapid method for doing frequency nondegenerate pump-probe spectroscopy which allows us to obtain data as in Fig. 7 very rapidly [13, 14].

White-Light Continuum (WLC) Pump-Probe Spectroscopy

Pump-probe methods have been used as NLO diagnostic tools for decades; however, spectroscopy has been minimal due to the difficulty of tuning the input sources. We developed a method for doing nonlinear absorption spectroscopy using a femtosecond pump along with a white-light continuum (WLC) femtosecond probe. This method was actually motivated by our work on nonlinear Kramers-Kronig (KK) relations for bound electronic nonlinearities [15–18]. What we found was that KK relations could be applied to frequency nondegenerate nonlinear absorption measurements to calculate the dispersion of the nondegenerate nonlinear refraction. The WLC pump-probe method is schematically shown in Fig. 9. Here a femtosecond pump beam prepares the sample to be interrogated by a broad spectrum pulse (WLC) that can

FIGURE 8
Linear absorption (right axis) and 2PA (left axis) vs wavelength for the molecule shown at the bottom. From Ref. [12].

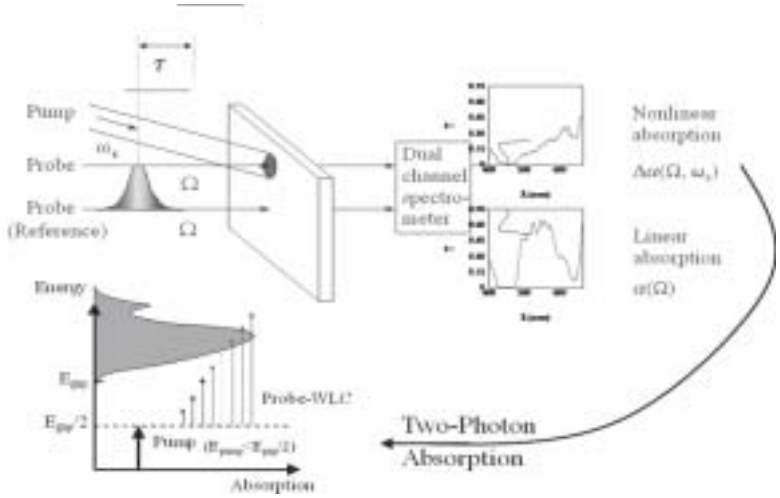

FIGURE 9
Femtosecond pump, white-light continuum probe spectroscopy setup showing the example of measuring 2PA.

be temporally delayed to give the spectral dynamics of the nonlinear absorption response. A WLC reference pulse gives the linear transmittance which can be subtracted from the transmittance of the probe WLC to give the change in transmittance at all wavelengths as a function of temporal delay [13]. These signals are detected either separately on a detector array or together on a dual detector array. This is a very powerful technique; however, it takes considerable skill to use and analyze data given that there are other ultrafast signals produced besides the nonlinear absorption signal that are described in detail in Ref. [14]. In the end, after the extraneous signals are removed, the data analysis can be fit with a single equation that depends on the chirp of the WLC, the sample's group-velocity dispersion (GVD), the pump irradiance, and of course the sample's nondegenerate nonlinear absorption. The GVD can be measured with the same apparatus by adding appropriate polarizers as in an optical Kerr effect measurement [19]. This pump-probe spectroscopic method has proven particularly useful for both 2PA and ESA and, given the temporal resolution, can easily distinguish between these nonlinearities [14]. Figure 10 shows data analogous to that shown in Fig. 8 but on a different molecule at different wavelengths [20]. The physical mechanism is the same as described for Fig. 7, i.e. solely nondegenerate 2PA with the pump at 1400 nm but followed by ESA for the pump at shorter wavelengths where it can induce 2PA by itself.

White-Light-Continuum Z-scan (WLC Z-scan)

The final technique we discuss is something we have been developing the last few years which we call white-light-continuum, WLC Z-scan [21–23].

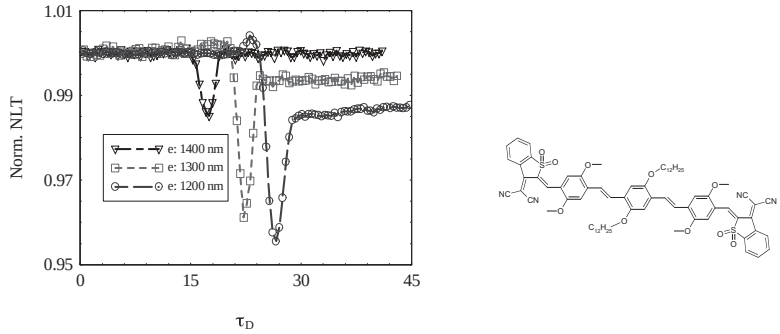

FIGURE 10
Data taken with the apparatus of Fig. 9 on the sample shown to the right. From Ref. [20].

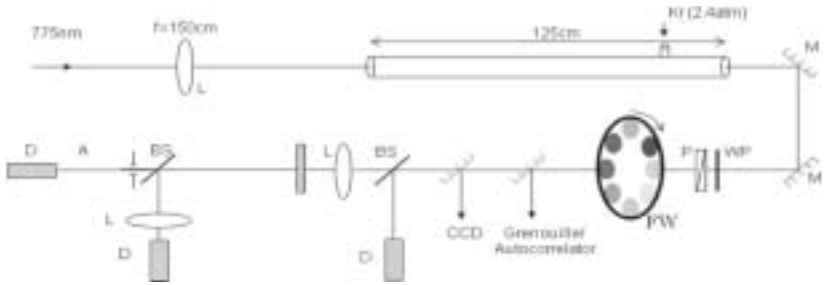

FIGURE 11
WLC Z-scan setup.

The basic idea is to produce a WLC strong enough to replace the source in the usual 'single' wavelength Z-scan [24, 25]. The apparatus is shown in Fig. 11.

The first thought would be to simply focus the entire WLC into the sample and scan it. Unfortunately this will lead to large nondegenerate nonlinearities as many different frequencies are simultaneously present within the sample, i.e. any $\omega_1 + \omega_2 = \mathrm{E}_{20}/\hbar$ will be absorbed in a 2PA process. We worked for some time to either temporally separate the different frequencies or to spatially separate them [21, 22], and while this can work, it is easiest to simply separate the different frequencies prior to the sample by narrow band filters [23]. However, the filters need to be broad enough to support the $\sim$100 fs pulses. Here $\sim$10 nm seems to work well, thus the color filter wheel is installed a shown in Fig. 11. The question can then be asked is, how is this any different from tuning an optical parametric device and using it as the input? The difference is significant in terms of the time it takes to measure the spectral dependence. For the WLC, its properties remain the same once fully characterized and do not change with turning the laser system on and off. We have found that we can obtain Gaussian spatial profile beams over an octave spectral

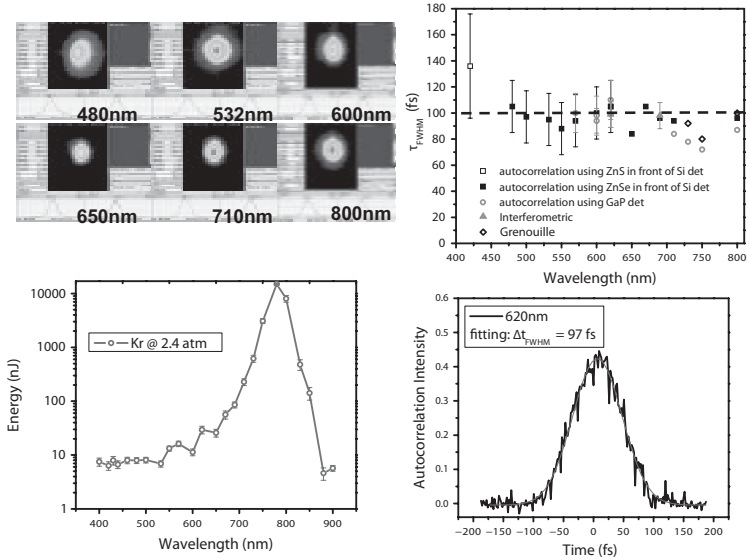

FIGURE 12
Characterization of the WLC. Spatial profiles – upper left, temporal pulsewidth -upper right, available energy after narrow band filters – lower left, example of an autocorrelation after a 620 nm narrow band filter (∼10 nm bandwidth – lower right) [23].

range – from 400 nm to 800 nm and the temporal duration is ∼100 fs over this entire range. Some of this characterization is shown in Fig. 12. A parametric device requires spatial filtering and constant tweaking necessitating continual, time-consuming characterization.

This WLC method has the potential of serving as the nonlinear equivalent of a spectrophotometer. With automation, we can imagine that a researcher could place a sample in the apparatus, push a button and then return sometime (perhaps < 1 hour) later to retrieve the degenerate nonlinear absorption spectrum; however, with this nonlinear spectrophotometer there is a bonus. The dispersion of the nonlinear refraction can be simultaneously measured by using a beam splitter and measuring the closed-aperture Z-scan as shown in Fig. 11. Using this configuration the data of Fig. 13 was taken.

MATERIALS

We have already given some examples of material nonlinearities in the preceding sections. A macromolecule that we have characterized quite fully is the porphyrin-squaraine-porphyrin molecule shown in Fig. 14. The linear and nonlinear spectra of the molecule and its components are shown in Fig. 15.

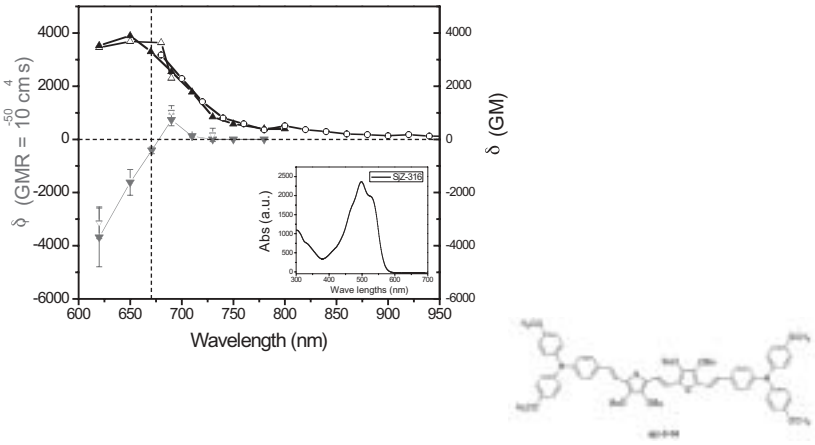

FIGURE 13
2PA cross section, right axis, and nonlinear refractive cross section, left axis for the molecule shown to the right [23]. Data taken using the WLC Z-scan, except for wavelengths longer then 800 nm where 2-photon fluorescence is used (open circles). From Ref. [23]

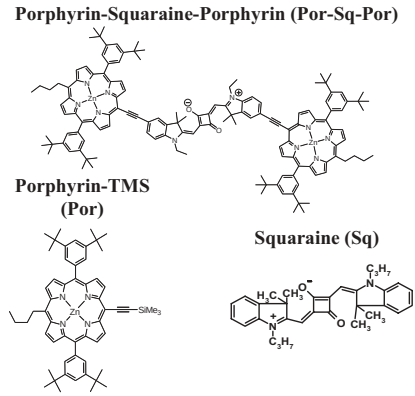

FIGURE 14
The porphyrin-squaraine-porphyrin with its component molecules shown below it.

It is interesting to note the very large enhancement of the macromolecule's 2PA compared with either of its constituents. The 2PA cross section is $>10^3$ GM over most of the octave range from an input wavelength of $\sim$1600 nm to 800 nm. These data were all taken with femtosecond pulses where instantaneous 2PA is dominant and values were checked to assure that ESA did not influence the values of α_2. Using picosecond pulses gives additional information. Figure 16 shows Z-scans taken at varying input energies for 29 ps pulses (FWHM) [26].

Using the energy level diagram and their corresponding propagation and rate equations of Fig. 17 allows us to fit the Z-scan data of Fig. 16. In fitting

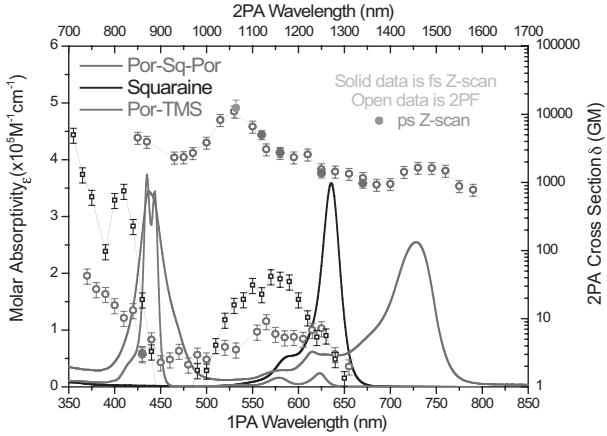

FIGURE 15
Linear absorption (left axis) and 2PA cross section (right axis) of the Por-Sq-Por molecule and its components. From Ref. [26].

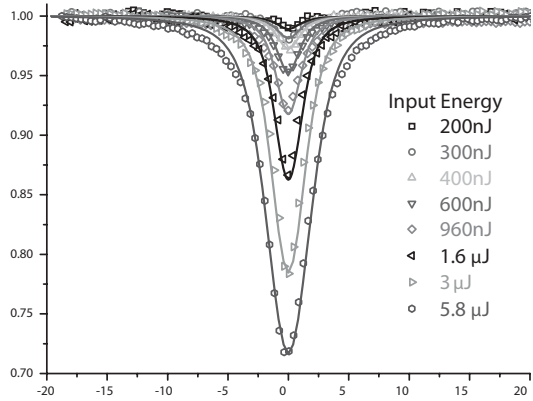

FIGURE 16
Z-scans of Por-Sq-Por for 1064 nm, 29 ps (FWHM) picosecond input. From Ref. [26].

this data, the values for α_2 (which gives the 2PA cross section σ_{01}) from the femtosecond data are used.

Figure 18 shows data and fits over a large input energy range for this molecule using 29 ps (FWHM), 1064 nm pulses which relies on values of molecular constants and 2PA obtained with femtosecond and picosecond Z-scan and pump-probe experiments. At the very highest input energies used, an additional set of higher lying levels, thus the 5-level system are included S_m see Ref. [26] for more details and justification.

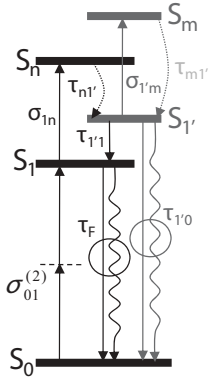

$$\frac{dI}{dz} = -\frac{\sigma_{01}^{(2)} N_0 I^2}{\hbar\omega} - \sigma_{1n} N_1 I - \sigma_{1'm} N_{1'} I, \text{ where } \alpha_2 = \frac{\sigma_{01}^{(2)} N_0}{\hbar\omega}$$

$$\frac{dN_0}{dt} = -\frac{\sigma_{01}^{(2)} N_0 I^2}{2(\hbar\omega)^2} + \frac{N_1}{\tau_F} + \frac{N_{1'}}{\tau_{1'0}}$$

$$\frac{dN_1}{dt} = \frac{\sigma_{01}^{(2)} N_0 I^2}{2(\hbar\omega)^2} - \frac{N_1}{\tau_F} - \frac{\sigma_{1n} N_1 I}{\hbar\omega} + \frac{N_{1'}}{\tau_{1'1}}$$

$$\frac{dN_{1'}}{dt} = -\frac{\sigma_{1'm} N_{1'} I}{\hbar\omega} + \frac{N_m}{\tau_{m1'}} + \frac{N_n}{\tau_{n1'}} - \frac{N_{1'}}{\tau_{1'1}} - \frac{N_{1'}}{\tau_{1'0}}$$

$$\frac{dN_n}{dt} = \frac{\sigma_{1n} N_1 I}{\hbar\omega} - \frac{N_n}{\tau_{n1'}}$$

$$\frac{dN_m}{dt} = \frac{\sigma_{1'm} N_{1'} I}{\hbar\omega} - \frac{N_m}{\tau_{m1'}}$$

FIGURE 17
5-level energy diagram and corresponding propagation and rate equations used to fit the Z-scans of Fig. 16 [26].

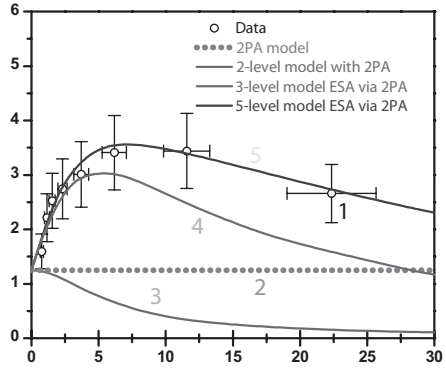

FIGURE 18
Effective 2PA cross section vs input irradiance of 1064 nm picosecond pulses. From Ref. [26].

We present data on this molecule over a very large irradiance range to show how complex the response can be; however, for ultrashort pulses at low input energies the results are relatively simple, i.e., α_2 and n_2 (data not shown) can describe the nonlinear interactions in the near IR. In addition, for relatively low input irradiances for picosecond pulses, only a single excited state needs to be included, e.g. below $\sim$4GW/cm^2 in Fig. 18. This is a common nonlinear response of organic materials in their transparency range (i.e. where 2PA is allowed but there is negligible linear absorption). It is in this regime where organic molecules respond in a manner similar to that observed for semiconductors. We make a comparison in the following section.

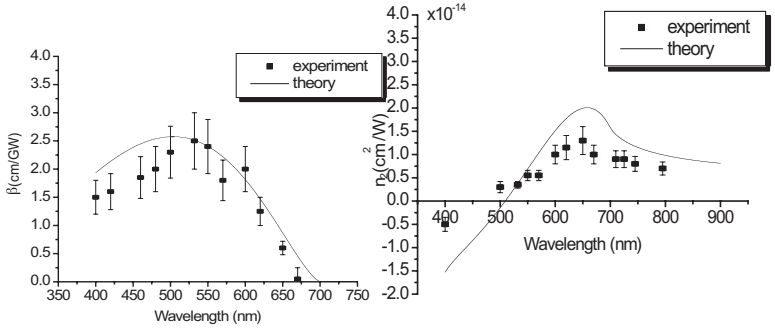

FIGURE 19
2PA coefficient (here β refers to $\propto_2$) of ZnS vs wavelength – left, and bound electronic nonlinear refractive index vs wavelength – right. See Ref. [23].

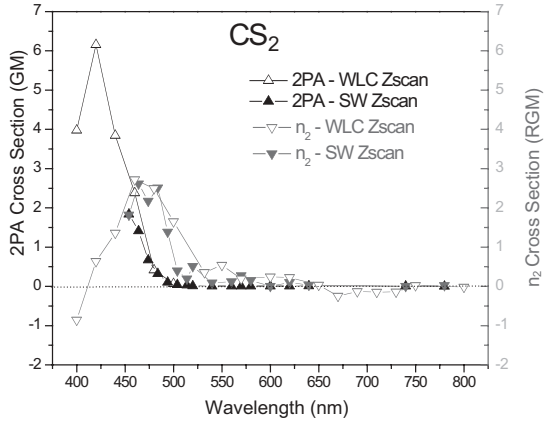

FIGURE 20
2PA cross section, open vertical triangles (left axis) and n_2, open triangles pointing down (right axis) for CS_2 using both single wavelength (SW) Z-scans and WLC Z-scans

Comparison of organic and semiconductor nonlinearities

A typical response for a semiconductor in the region where 2PA is observed is shown in Fig. 19. Looking back at the data for the organic dye of Fig. 13, we see a striking similarity to the data for ZnS in Fig. 19, i.e. there is a peak near the peak of the 2PA and then it turns negative for shorter wavelengths. Interestingly the same trend can be seen in the simple CS_2 molecule as shown in Fig. 20. The primary difference appears to be in the width of the 2PA transition, much broader for semiconductor absorption bands, as well as the 'width' of the nonlinear refraction features. This is expected due the connection between index and absorption through Kramers-Kronig relations except we are looking here at the degenerate nonlinearities for which the relations do not apply directly [18].

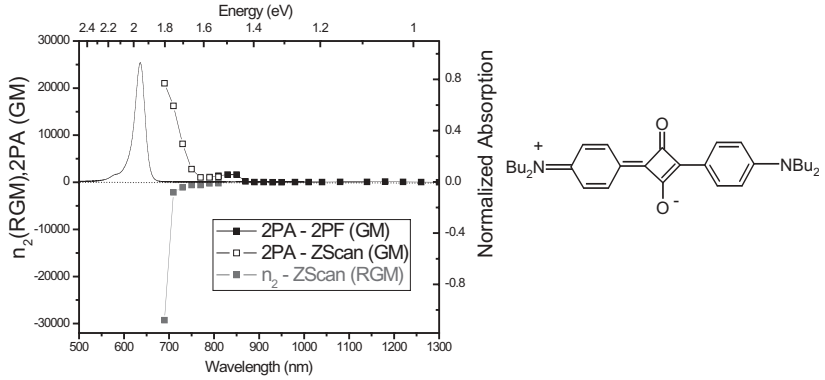

FIGURE 21
Linear absorption (solid black line), nonlinear absorption (black squares) and nonlinear refraction (red squares) for molecule at right.

It is also interesting to look at the relative values of the nonlinear refraction and nonlinear absorption. One way to do this is to look at the ratio

$$\frac{k_0 n_2{}^{\max}}{\alpha_2^{\max}} = \frac{1}{2}\frac{\mathrm{Re}\chi^{(3)}|^{\max}}{\mathrm{Im}\chi^{(3)}|^{\max}} = \frac{\delta_R^{\max}}{\delta^{\max}}, \tag{7}$$

where these are the maximum values of the cross sections which occur at different wavelengths. This ratio is the usual all-optical switching ratio if the cross sections are evaluated at the same wavelength [27]. Here the maximum of 2PA and n_2 are shifted in frequency by ∼150 nm for semiconductors and ∼50 nm for the molecule of Fig. 13 and ∼50 nm for CS_2. For the semiconductor ZnS this ratio is ∼1/2 and for ZnSe it is ∼3/4. For the molecule of Fig. 13 the ratio is ∼1/4 and for CS_2 it is ∼1/2, i.e., the order of unity for all of these materials.

However, Fig. 21 shows a squaraine molecule where the nonlinear refraction is qualitatively different. There the positive peak in n_2 at wavelengths on the red side of the 2PA peak is missing. We suspect that this is due to the dominance of the quadratic Stark effect (so-called negative term) for this molecule. Looking at the nonlinear refraction for a simple 3-level system far from resonance we have [9]:

$$n_2 = 3\frac{Nf^{(3)}}{n^2\varepsilon_0^2 c\hbar^3\bar{\omega}_{g1}^3}\left\{\frac{\bar{\omega}_{g1}}{\bar{\omega}_{g2}}|\bar{\mu}_{g1}|^2|\bar{\mu}_{21}|^2 - |\bar{\mu}_{g1}|^2|\bar{\mu}_{g1}|^2\right\} \tag{8}$$

where $f^{(3)}$ is a local field correction term and other quantities are defined similarly to those for Fig. 5 [9]. The second term is the so-called negative term which is often called 'virtual saturation' since this term smoothly goes to real saturable absorption above resonance. These two terms are depicted

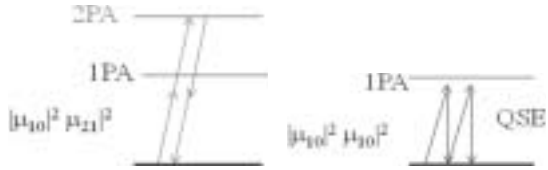

FIGURE 22
Sketch showing the two terms in Eq. 6 due to 2PA, left; and quadratic-Stark effect, QSE, right.

in Fig. 22. In semiconductors both 1PA and 2PA are allowed between the valence and conduction band so that the energy difference between the one-photon allowed state and the two-photon allowed state is fixed at zero. In organic materials the one and two-photon allowed states can be separately tuned via molecular engineering. This allows some flexibility in changing the relative values of the terms in Eq. 6 as well as adding an additional term for molecules with permanent dipole moments. There is considerable discussion of this flexibility in terms of bond-length alternation, BLA, in the organics literature [28, 29].

In addition to the comparisons of 2PA spectra and n_2 dispersion between organic dyes and semiconductors, there are also analogous higher-order nonlinearities associated with both materials [5]. In semiconductors, 2PA generated free carriers gives a fifth-order nonlinear absorption that is directly analogous to 2PA-generated excited-state absorption in organics [30]. Additionally 2PA-generated free-carrier refraction (again a fifth–order response) is analogous to the excited-state refraction from 2PA-generated excited states in organics; however, while free-carrier refraction is always negative, either sign is possible for excited-state refraction since they are not ‘free’, i.e. not zero-frequency oscillators.

CONCLUSION

We have examined a variety of methods for determining the nonlinear optical response of organic materials. Any single experiment is unlikely to be able to unravel all of the different nonlinear mechanisms active in a material on various time scales. Ultrafast nonlinearities often require femtosecond resolution to unambiguously determine their sign and magnitude. For longer pulses other effects such as excited-state absorption and refraction can become significant and can even dominate the nonlinear response. These nonlinearities are reminiscent of similar nonlinearities in semiconductors where free-carrier effects take the place of excited-state effects. However, unlike in semiconductors where the band structure determines the response, in organics the individual molecular levels can be moved via molecular engineering giving some potential ability to tune the nonlinear response. On the other hand, nonlinearities

are still not as large as is desirable for many of the potential applications for all-optical switching and optical limiting.

ACKNOWLEDGEMENTS

We wish to thank the U. S. Army Research Office under contract/grant number 50372-CH-MUR and National Science Foundation ECS 0524533 and many other funding agencies over the years. EVS also thanks all of his colleagues, postdocs and students who have contributed greatly to this research.

REFERENCES

[1] M. Sheik-bahae, A. A. Said, and E. W. Van Stryland. High sensitivity, single beam n_2 measurements. *Opt. Lett.* **14** (1989), 955–957.

[2] M. Sheik-bahae, A. A. Said, T. H. Wei, D. J. Hagan, and E. W. Van Stryland. Sensitive measurement of optical nonlinearities using a single beam. *Journal of Quantum Electronics* **JQE QE-26** (1989), 760–769.

[3] Most cited article from IEEE JQE, in IEEE LEOS News Letter, page 17–29, Feb. 2007.

[4] T. Xia, D. J. Hagan, M. Sheik-Bahae, and E. W. Van Stryland. Eclipsing Z-scan measurement of $\lambda/10^4$ wavefront distortion. *Opt. Lett.* **19** (1994), 317–319.

[5] A. A. Said, C. Wamsley, D. J. Hagan, E. W. Van Stryland, B. A. Reinhardt, P. Roderer, and A. G. Dillard. Third and fifth order optical nonlinearities in organic materials. *Chem. Phys. Lett.* **228** (1994), 646–650.

[6] J. Chung, S. J. Zheng, T. Odani, L. Beverina, J. Fu, L. A. Padilha, A. Biesso, J. M. Hales, X. Zhan, K. Schmidt, A. Ye, E. Zojer, S. Barlow, D. J. Hagan, E. W. Van Stryland, Y. Yi, Z. Shuai, G. A. Pagani, J. L. Bredas, J. W. Perry, and S. R. Marder. Extended squaraine dyes with large two-photon absorption cross-sections. *J. Am. Chem. Soc.* **128** (2006), 14444–14445.

[7] E. W. Van Stryland and M. Sheik-Bahae. Z-Scan, in Characterization techniques and tabulations for organic nonlinear optical materials, 655–692, Mark Kuzyk, Carl Dirk and Marcel Decker (eds.) (1998). Also see. Measuring nonlinear refraction and its dispersion via propagation. E. Van Stryland and D. Hagan, chapter in Self-focusing: Past and Present. Springer Topics of Applied Physics Series, Robert Boyd, Svetlana Lukishova, Ron Shen (ed.), Springer Verlag, 2007.

[8] T. H. Wei, D. J. Hagan, M. J. Sence, E. W. Van Stryland, J. W. Perry, and D. R. Coulter. Direct measurements of nonlinear absorption and refraction in solutions of phthalocyanines. *Appl. Phys. B* **54** (1992), 46–51.

[9] Demetrios N. Christodoulides, Iam Choon Khoo, Gregory J. Salamo, George I. Stegeman and Eric W. Van Stryland. Nonlinear refraction and absorption: Mechanisms and magnitudes. to be published in Advances in Optics and Photonics, 2010.

[10] For example, see, Picosecond Phenomena. C. V. Shank, E. P. Ippen, and S.L. Shapiro (Eds.), Springer–Verlag, 1978.

[11] S. Webster, J. Fu, L. A. Padilha, O. V. Przhonska, D. J. Hagan, E. W. Van Stryland, M. V. Bondar, Y. L. Slominsky and A. D. Kachkovski. Comparison of nonlinear absorption in three similar dyes: Polymethine, squaraine and tetraone. *Chem. Phys.* **348** (2008), 143–151.

[12] Topics in Fluorescence Spectroscopy, vol. 5: Nonlinear and Two-Photon Induced Fluorescence, Joseph R. Lakowicz (ed.), Springer, 1997.

[13] Raluca Negres, Joel Hales, Andrey Kobyakov, David Hagan, and Eric Van Stryland. Two-photon spectroscopy and analysis with a white-light continuum probe. *Optics Letters* **27** (2002), 270–272.

[14] Negres, R. A., Hales, J. M., Kobyakov, A. K., Hagan, D. J., Van Stryland, E. W. Experiment and analysis of two-photon absorption spectroscopy using a white-light continuum probe. *IEEE* **JQE 38**(9) (2002), 1205–1216. Also see erratum, R. A. Negres, J. M. Hales, A. Kobyakov, D. J. Hagan, E. W. Van Stryland. *IEEE* **JQE 39**(2) (2003), **392**.

[15] M. Sheik-Bahae, D. J. Hagan, and E. W. Van Stryland. Dispersion and band-gap scaling of the electronic Kerr effect in solids associated with two-photon absorption. *Phys. Rev. Lett.* **65** (1989), 96–99.

[16] F. Bassani, and S. Scandolo. Dispersion relations and sum rules in nonlinear optics. *Phys. Rev. B* **44** (1991), 8446–8453.

[17] M. Sheik-Bahae, D. C. Hutchings, D. J. Hagan, and E. W. Van Stryland. Dispersion of bound electronic nonlinear refraction in solids. *JQE*, **QE-27** (1991), 1296–1309.

[18] D. C. Hutchings, M. Sheik-Bahae, D. J. Hagan, and E. W. Van Stryland. Kramers-kronig relations in nonlinear optics. *Optical and Quantum Electronics* **24** (1992), 1–30.

[19] Yamaguchi and H. Hamaguchi. Convenient method of measuring the chirp structure of femtosecond white-light continuum pulses. *Appl. Spectroscopy* **49** (1995), 1513–1515.

[20] Sample from Seth Marder, unpublished data.

[21] M. Balu, J. Hales, D. Hagan, and E. Van Stryland. White-light continuum Z-scan technique for nonlinear materials characterization. *Optics Express* **12** (2004), 3820–3826.

[22] Mihaela Balu, Joel Hales, David J. Hagan, and Eric W. Van Stryland. Dispersion of nonlinear refraction and two-photon absorption using a white-light continuum Z-scan. *Optics Express* **13** (2005), 3594–99.

[23] M. Balu, L. Padilha, D. Hagan, E. Van Stryland, S. Yao, K. Belfield, S. Zheng, S. Barlow, and S. Marder. Broadband Z-scan characterization using a high-spectral-irradiance, high-quality supercontinuum. *JOSA B* **25** (2008), 159-165. Also see erratum, M. Balu, L. Padilha, D. Hagan, E. Van Stryland, S. Yao, K. Belfield, S. Zheng, S. Barlow, and S. Marder. Broadband Z-scan characterization using a high-spectral-irradiance, high-quality supercontinuum-erratum. *JOSA B* **26** (2009), 1663.

[24] P. B. Corkum, C. Rolland. Supercontinuum generation in gases. *Phys. Rev. Lett.* **57** (1986), 2268–2271.

[25] K. Sokolowski-Tinten, K. Werner, M. Zhou, and D. Von Der Linde. Femtosecond continuum generation using a gas-filled hollow fiber. CLEO Conference, Baltimore, May 23–28, 1999.

[26] S. Webster, S. A. Odom, L. A. Padilha, O. V. Przhonska, D. Peceli, H. Hu, G. Nootz, A. D. Kachkovski, J. D. Matichak, S. Barlow, S. R. Marder, H. L. Anderson, D. J. Hagan, and E. W. Van Stryland. Linear and nonlinear spectroscopy of a porphyrin-squaraine-porphyrin conjugated system. *J. Phys. Chem. B*, In Press: DOI: 10.1021/jp904460f (2009).

[27] V. Mizrahi, K. W. DeLong, and G. I. Stegeman. Two-photon absorption as a limitation to all-optical switching. *Opt. Lett.* **14** (1989), 1140–1142.

[28] D. Lu, G. Chen, J. Perry, W. Goddard III. Valence-bond charge-transfer model for nonlinear optical properties of charge-transfer organic molecules. *J. Am. Chem. Soc.* **116** (1994), 10679–10685. See also, F. Meyers, S. MArder, B. Pierce, J. L. Bredas, Electric field modulated nonlinear optical properties of donor-acceptor polyenees: sum-over-states investigation of the relationship between molecular polarizabilities (α, β and γ) and bond length alternation. *J. Am. Chem. Soc.* **116** (1994), 10703–10714.

[29] S. Marder, B. Kippelen, A. Jen, N. Peyghambarian. Design and synthesis of chromophores and polymers for electro-optic and photorefractive applications. *Nature* **388** (1997), 845–851.

[30] A. A. Said, M. Sheik-Bahae, D. J. Hagan, T. H. Wei, J. Wang, J. Young and E. W. Van Stryland. Determination of bound and free-carrier nonlinearities in ZnSe, GaAs, CdTe, and ZnTe. *JOSA B 9* (1992), 405-414.